Real time control of the plasma current and elongation in tokamaks using ECRH actuators

J I Paley, S Coda and the TCV Team

Ecole Polytechnique Fédérale de Lausanne (EPFL), Centre de Recherches en Physique des Plasmas, Association Euratom-Confédération Suisse, CH-1015 Lausanne, Switzerland

Email: james.paley@epfl.ch

Abstract. Real time control of the plasma elongation and plasma current using electron cyclotron resonance heating (ECRH) actuators has been demonstrated on TCV. Tokamak plasmas may be elongated by off-axis ECRH. The associated flattening of the current density profile increases the plasma's vertical stability, enabling higher elongations to be obtained, at lower currents than would be possible in Ohmic conditions. Successful experiments were carried out on TCV to control, in real time, the magnitude of the elongation and the ECRH deposition location using second harmonic ECRH power and ECRH launcher mirror angle actuators. Plasma current control in fully non-inductive plasmas using ECRH actuators to drive ECCD was also demonstrated.

Pacs numbers. 45.80.+r,52.50.Sw,52.55.–s,28.52.–s,52.55.Fa,52.70.Ds
Submitted to. Plasma physics and controlled fusion

1. Introduction

Electron cyclotron resonance heating (ECRH) systems can provide plasma heating and current drive, assist with plasma start-up and control MHD activity, such as neoclassical tearing modes (NTM) and sawteeth in tokamak plasmas. NTMs are stabilised by driving current (ECCD) on the resonant flux surface associated with the NTM [1,2]. Real time control of ECRH systems is required for NTM control as it is necessary to track the position of the resonant flux surface and ensure the ECRH beam power is absorbed precisely at this flux surface. It may also be necessary in future devices to control the ECRH power from multiple, toroidally separated launchers in phase with the rotating NTM, such that the ECRH is only absorbed at the O-point [3,4]. DIII-D and FTU have successfully demonstrated real time control of NTM activity using fixed ECRH mirrors, instead varying the plasma major radius, plasma current or toroidal field such as to focus the ECRH beam onto the magnetic island and in FTU by operating gyrotrons focussed on different positions [5,6]. In ITER these parameters will be set by requirements other than NTM control and therefore steerable mirrors will be required to track the NTM. This has been demonstrated on JT-60U where steerable mirrors were used to stabilise NTMs [7]. The ITER upper launcher ECRH system will be used primarily for NTM stabilisation and elimination [8] and will have multiple real time steerable mirrors [9].

The ability to control ECRH actuators, and particularly heavy moving parts such as mirrors, in real time is therefore crucial to the operation of ITER and needs to be demonstrated in the current

generation of fusion experiments. To this end, previous experiments to control the angle of the 3rd harmonic ECRH launcher on TCV [10] have been extended to demonstrate control of the 2nd harmonic, multi-launcher mirror angles and ECRH power level.

The plasma elongation (κ) in a tokamak is generally controlled by the quadrupole magnetic field generated by the poloidal magnetic field shaping coils. However the elongation also has a dependence on the plasma current profile, ie the internal inductance (l_i). Specifically, reducing the internal inductance, i.e. broadening the current profile, results in an elongation increase. A broadening of the current profile can be effected by heating the plasma off-axis, which depresses the resistivity locally and under an applied loop voltage, draws more current to the outer part of the plasma; therefore in a constant quadrupole (and hexapole) poloidal magnetic field, heating off-axis elongates the plasma. This was first demonstrated on TCV by Pochelon et al. [11]. In this way, highly elongated (κ~2.4), low current (I_N ~1) plasmas were generated that would otherwise be vertically unstable in purely Ohmic plasmas.

During the ECRH phase, the plasma height increases and given that the plasma centre remains stationary and the ECRH is absorbed above the plasma centre, the ECRH deposition profile moves to lower ρ[1], reducing the off-axis current and saturating the elongation effect. In the previous experiments by Pochelon et al. [11], the ECRH mirrors were moved during the pulse in an attempt to maintain the ECRH deposition at constant ρ, maximising the obtained elongations. A simple feedforward waveform was provided to the mirror position controller to achieve this. We have developed a real time feedback control mechanism to track the ECRH deposition at constant ρ and a second algorithm to control the magnitude of the elongation (κ between 1.7 and 2.2) using the ECRH mirror angle and power actuators, respectively.

The plasma current in tokamaks is usually provided by the magnetic induction from Ohmic transformer coils. Current may also be driven in plasmas by pressure gradients (bootstrap current) and wave current drive, for example electron cyclotron current drive (ECCD) – current provided by electron cyclotron waves. In TCV fully non-inductive operation is achieved routinely, relying primarily on ECCD [12,13]. In this mode of operation the current in the Ohmic transformer primary is clamped to a constant value to ensure no external inductive voltage injection. Real time control of the plasma current using ECRH actuators in fully non-inductive current scenarios (zero loop voltage) has been demonstrated on TCV, providing control of ~30kA of plasma current (in ~160kA discharges) with up to 2.7MW of ECRH power.

2. Experimental setup

2.1. TCV ECRH systems

TCV (major radius 0.88m, toroidal field = 1.5T, max current = 1MA, elongation up to κ = 2.8) is uniquely placed to explore real time control of ECRH with its highly flexible ECRH systems [14]. The 4.5MW TCV ECRH setup consists of 6 gyrotrons operating at the 2nd harmonic in X-mode (82.7GHz - X2) delivering up to 3MW and 3 gyrotrons operating at the 3rd harmonic (118GHz - X3) providing 1.5MW. Real time control of the X3 mirrors has previously been demonstrated by S. Alberti et al. [10] where the strong dependence of X3 absorption on mirror position necessitates the

[1] Where ρ is defined as a volume function throughout this article as $\rho \sim \sqrt{V/V_{LCFS}}$ where V_{LCFS} is the volume enclosed by the last closed flux surface.

implementation of feedback control of the mirror angle to maintain strong absorption in the plasma. There are two independent power supplies for the X2 gyrotrons, allowing the power level of each group of 3 X2 gyrotrons to be controlled in real time. A matching optics unit at the output of the gyrotrons enables any desired polarisation and, in the experiments described herein, ensures the output is X mode (no real time control). Evacuated waveguides lead to the tokamak and each waveguide is terminated by an independent system of mirrors, the ECRH launchers [15], as shown in Figure 1. The whole launcher rotates along its longitudinal axis to control the ECRH beam orientation in the toroidal direction and the final mirror rotates to control the poloidal deposition location. The two motions are conventionally termed ‘toroidal’ and ‘poloidal’, respectively, but in general each affects both the parallel wave number and the deposition location. The motion is driven by a system of push-rods, springs and stepper motors. Only the ‘poloidal’ axis is currently controllable in real time during a shot. The motors are each controlled by an independent PID controller, minimising the error between the requested and measured mirror position.

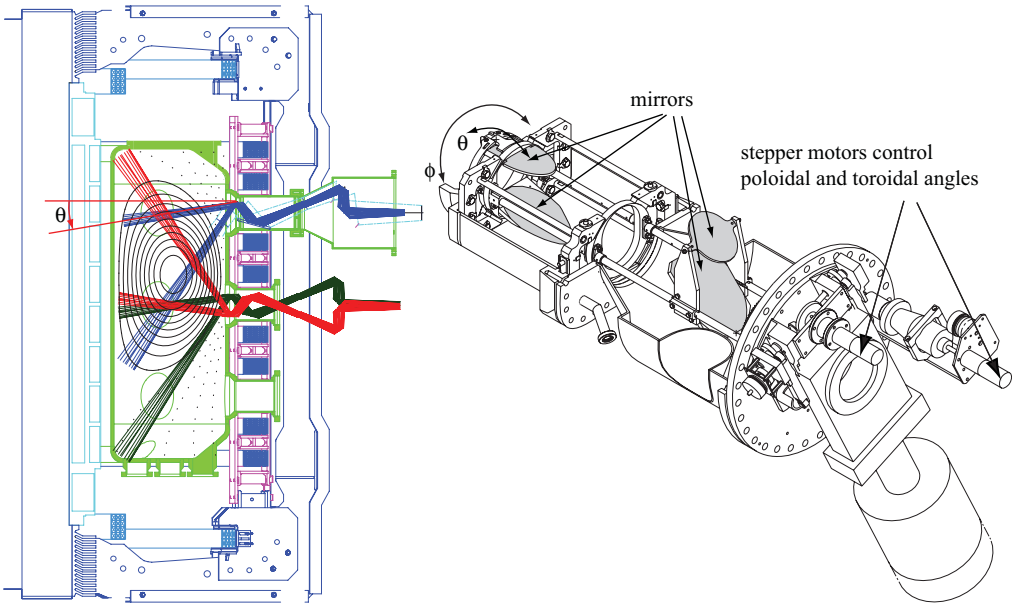

Figure 1 left. Poloidal plane view of the X2 upper launcher and the ECRH beam’s range of ‘poloidal’ angles for both the upper and equatorial launchers. From the flux contours in this diagram and for a constant shallow mirror angle at the upper launcher, it is clear that as the plasma elongates the ECRH deposition would move towards the plasma core. Feedback control of this angle would be required to track the deposition location. Right. The X2 ECRH launcher system. The final mirror turns in the ‘poloidal’ direction and the whole system turns on its longitudinal axis in the ‘toroidal’ direction as is shown on the left for the equatorial beams.

The mechanics of the launchers limits the range of poloidal angles available for any given ‘toroidal angle’. Care was taken with our design for the elongation controller such that these limits were not reached as ‘sticking’ or even damage may result – see section 2.2.

2.2. Controller setup

TCV uses a hybrid analogue/digital control system [16,17] to control the plasma parameters in real time. It is based on matrix multiplication of signals and a PID controller: a diagram is shown in Figure 2. Up to 128 inputs are fed into the initial A matrix which calculates the observables such as plasma current, position, elongation, coil currents and density. Error signals are generated by subtraction of

the A matrix outputs from reference signals generated in wave generator B. After a programmable amplifier, a PID controller operates on the error signals and the result is fed into the G matrix where the required actuator signals are calculated. The G matrix also selects the terms required from the PID controller (eg proportional or proportional-integral etc). In the case of coil currents, the G matrix calculates the coil voltage increments, which are then corrected for finite coil resistivity and for the mutual coupling between coils in the M matrix. All the signals are then summed with feedforwards and the 20 outputs fed to actuators (power supplies and a gas valve). All the matrix coefficients can be changed during a shot at a number of pre-defined times by the digital controller.

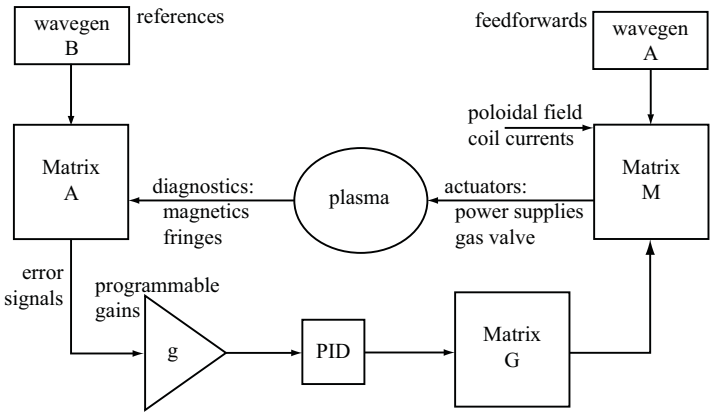

Figure 2: The TCV hybrid controller is based on linear matrix multiplication of signals and a PID controller. The A matrix elements may take values up to +/-0.5. The programmable gains (P) may take factors 1,2,4,8. G matrix and M matrix up to +/-2.0. Signals within the controller are limited to about +/-10V.

Usually all the controller channels are required in the nominal plasma control loop. In our experiments, some of the shaping coil feedback loops were removed from the controller and placed in their own feedback loops internal to their power supplies. This freed up channels in the controller to be used for control of the ECRH systems at the expense of having reduced control of the feedback gains for the particular coil – the PID gains are set manually in the power supply controllers. It is necessary to prevent the controller signals saturating with voltages much larger than +/-10V, otherwise the controller response becomes unpredictable and artefacts are observed in the outputs, including cross-talk between signals. Therefore the system gains must be designed with this in mind.

2.3. Elongation control

2.3.1. *Elongation observable.* For control loops based on the plasma elongation, a real time measurement of the elongation ($\kappa_{realtime}$) is necessary. Unfortunately TCV has no real time equilibrium reconstruction that could be used for such a purpose. Instead an approximate observable was generated based on a finite element model of the plasma as described in the Appendix. This real time elongation is most accurate in the case when other plasma parameters, eg position, current and triangularity remain approximately constant. The finite element model calculates the required linear combinations of the magnetics signals, the coefficients of which are entered into the A matrix to calculate $\kappa_{realtime}$.

2.3.2. *Elongation control algorithm*. The $\kappa_{realtime}$ signal is used in an algorithm to control the magnitude of the plasma elongation, which consists of a simple proportional and integral controller. The calibration of $\kappa_{realtime}$ to elongation was done by running experiments in open-loop, whereby the

gyrotrons are switched on at full power and $\kappa_{realtime}$ compared to the elongation calculated post-shot using the equilibrium reconstruction code LIUQE[18]. The required reference signal was then constructed.

The M matrix could be conveniently employed as a hardware protection element such that when the maximum/minimum input voltage to the M matrix is attained (~+/-10V), the M output stays with a defined voltage range for safe operation of the gyrotron power supplies. For example, selection of an M matrix gain of 0.5, together with feedforward signal of 2V (which is simply summed with the M matrix output) will provide an absolute maximum voltage range on the actuator of -3V to 7V. All the equipment on TCV is designed to be ultimately self-protecting and an input over-voltage will thus result in a fast power supply shutdown, terminating operation for the remainder of the shot. In addition, this can also be accompanied by gyrotron arcs, requiring subsequent reconditioning and loss of operational time. At the other extreme, under-voltage causes the gyrotron output to effectively go to zero and the energy of the electron beam to be channelled entirely as heat on the gyrotron collector, which should be avoided and indeed also eventually leads to a shutdown. The M matrix coefficients together with the feedforward power trace were set such as to maintain the gyrotron cathode voltage within this range (equivalent to a controllable output power of 200 to 450kW per gyrotron, with the feedforward equivalent to 270kW). Both proportional and integral control were used in the elongation control algorithm, with integral control required, as expected, to minimise the steady state error.

Sufficient off-axis plasma density is required to provide good (~60%) first pass absorption of the ECRH beam. Initial experiments failed to obtain high elongation as the off-axis density was too low. In these cases it was also possible that the EC wave was reflected on the centre column of the device and the remaining ECRH energy deposited in the plasma core, inhibiting the flattening of the current profile. Increasing the density before ECRH switch-on revealed the existence of a critical density (n_e~2x$10^{19}$$m^{-3}$ at the location of the ECRH deposition; ρ~0.7) above which high elongations were obtained. During the ECRH phase, the electron density rapidly decreases due to increased wall pumping from the larger surface wetted by the higher-elongated plasma [11], therefore reducing the absorption.

2.3.3. Deposition tracking algorithm. A prediction on the mirror angle required to maintain the ECRH deposition at constant ρ was obtained from the geometry of the plasma-mirror system at ECRH switch on (κ=1.7) and at maximum elongation (κ=2.2) and also by running the TORAY-GA [19] ray tracing code to obtain the deposition profiles for various mirror angles. The estimate of the mirror angles required to maintain the ECRH deposition at ρ=0.7 for κ=1.7 and κ=2.2 was then used to obtain the following linear relationship between the elongation (or the $\kappa_{realtime}$ signal voltage) and the mirror angle (or required mirror motor voltage V_{mirror}).

$$V_{mirror} = C\kappa_{realtime} + D \qquad (2.1)$$

The controller matrices and wave generators of the controller were used to construct the proportional and offset factors (constants C and D) in this linear relationship as shown in Figure 3 and given below.

$$C = gPGM \qquad (2.2)$$

$$D = wave_A - (gPGM)\, wave_B \qquad (2.3)$$

Both signal generators are set to constant voltage with $wave_B$ used to shift the voltage of the controller signals within the available range of +/-10V. Two launchers were used in these experiments, each with a slightly different mirror-angle to V_{mirror} calibration and therefore they required a slightly different selection of the constants *C* and *D* in the above equations, to impose the mirrors at all times to the same angle.

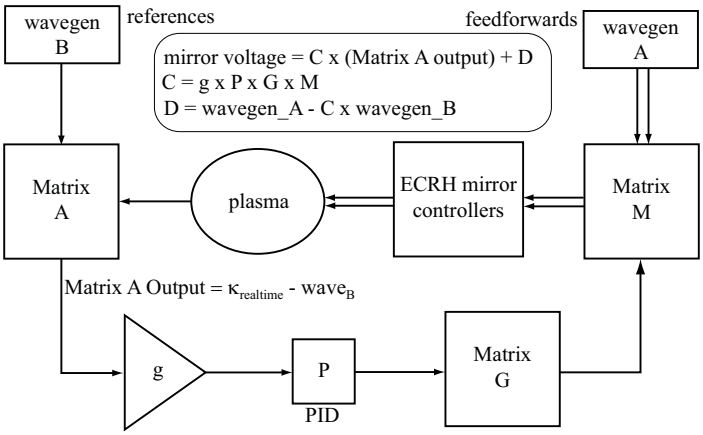

Figure 3. Block diagram of the TCV controller adapted for the deposition tracking control experiments. The elongation controller uses a similar method in addition to integral control.

The available 'poloidal' angle range of the mirror is limited by the mechanics of the launcher, and has a minimum value of ~6 deg. It is judicious to prevent the controller driving the mirror to such low angles as there is a finite chance that the mirror could become stuck or damaged. This was done again by imposing an appropriate low gain on the M matrix, and concomitantly selecting the appropriate feedforwards. At saturation of the input to the M matrix (~+/-10V), the controller limits the mirrors to the required angle range.

2.4. Plasma current control algorithm

The plasma current controller was setup in a similar fashion. The plasma current observable was provided by the usual real time calculation of the current in the A matrix, typically used for current control using the Ohmic coils. The Ohmic coils were set to provide zero loop voltage during the ECRH phase (provided by imposing a constant current in the coils; controlled by the coil power supplies). The mirror angles were held constant with sufficient toroidal angle as to provide wave current drive and the gyrotron power level controlled by the TCV controller output. Again the M matrix and feedforward signal was used to limit the gyrotron cathode voltage to a pre-defined range and the programmable gains and G matrix values set to appropriate values, avoiding saturation of the controller signals as far as possible. With all 6 X2 gyrotrons in operation a controllable power range from 1.2 to 2.7MW was available.

An initial open-loop experiment was carried out to determine the reference current level for a given heating power, from which the closed-loop reference current trace could be designed. Step and flat references were tested, initially using proportional control and followed by both proportional and integral control. The ECRH launchers were fixed in position throughout the ECRH power feedback phase.

3. Results.

3.1. Elongation control

From 0.3s to 1.5s ECRH from two gyrotrons was applied to a target plasma (L-mode, I_p=300kA) of elongation κ=1.7 with the quadrupole and hexapole shaping fields held constant. Figure 4 left shows the currents in each of the shaping coils (labelled sets E and F) were approximately constant during the constant power ECRH phase and therefore the change in elongation follows from the current profile modification. Further confirmation is provided by Figure 4 right which shows the changes in the coil currents required to reduce the elongation (in fact there was feedback control of the elongation in this pulse in a failed attempt to maintain the elongation against the pre-programmed coil currents and therefore the ECRH power increases slightly from 1.0s, but the effect of the coils is much larger than the ECRH). The EC waves were injected with zero toroidal angle and therefore no electron cyclotron current drive exists; the current change was entirely due to modification of the plasma resistivity. (The additional current that can be driven by current drive is rather modest at this outer location, owing to the low temperature [20], and steering the mirror only in the poloidal plane greatly simplifies the experiment.)

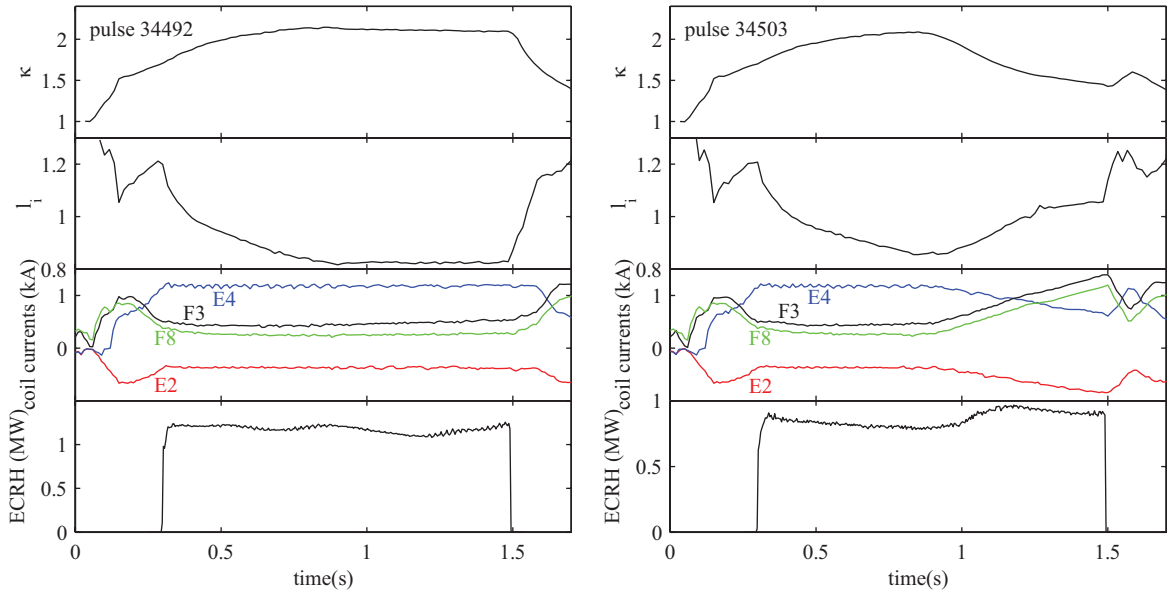

Figure 4 left. Open loop application of ECRH under constant quadrupole field. Shown are a selection of poloidal field shaping coil currents which are broadly constant during the elongation phase (0.3 to 1.5s). The l_i is also shown. Right. Introducing a decrease in the pre-programmed elongation by feedforward control of the coil currents at 0.9s.

The two elongation control algorithms were first tested separately: Initially experiments were performed to control the magnitude of the elongation using feedback control of the ECRH power, using only proportional control and with the controller gains set as large as possible. Flat, step-up and step-down elongation reference signals were tested. Flat and step-down references behaved as expected. A step-down control experiment is shown in Figure 5. There was insufficient ECRH power in this pulse to achieve the initial elongation reference (κ~2.4) which was not helped by over-voltage in the controller preventing the ECRH power obtaining maximum power until t~0.4s, but the elongation settles to the lower reference in ~200ms after the programmed step-down. This occurs because the off-axis current drive is reduced and the current profile becomes more centralised, which should occur in a current redistribution time ~150ms on TCV and is consistent with the observed response. The addition of integral control, together with modifying the gains to prevent over-voltage

should allow a higher initial elongation to be achieved. There was a slight drop in the elongation at 0.9s, before the pre-programmed step-down, which is due to the TCV Ohmic coil current passing through zero and changing sign, causing a slight perturbation in coil currents and in the plasma shape. The temporal proximity of this event to the step-down is purely coincidental. There was a poor response, however, to step-up references as the plasma density rapidly decreases during the initial ECRH phase, giving poor absorption in the outer plasma at the time of the step-up and therefore only mildly elongated plasmas (κ~1.8-1.9) could be obtained.

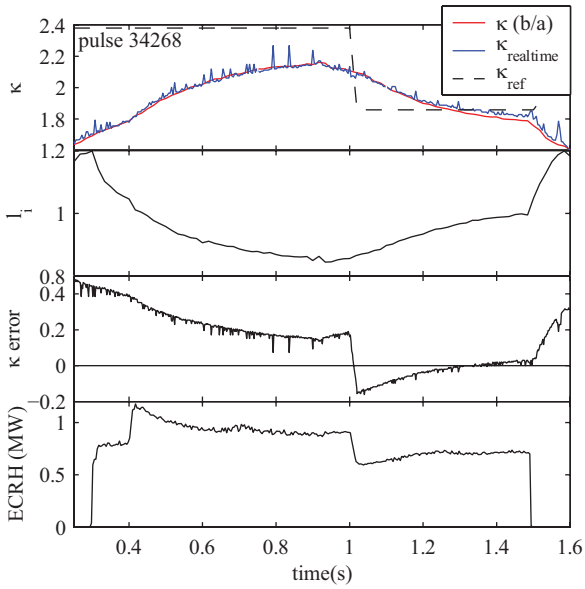

Figure 5. Real time control (proportional only) of the plasma elongation. At the step-down in the elongation reference, the power is reduced and the elongation responds as expected. There was insufficient power to achieve the initial high elongation reference.

3.2. Elongation and deposition tracking control

After testing the deposition tracking algorithm with open-loop control on the elongation magnitude, both control algorithms were applied simultaneously – see Figure 6. Integral control was added to the elongation magnitude algorithm. The reference elongation signal was set to roughly κ=2.1 with a step down to κ=1.8 at time 1.0s. Two gyrotrons were again used together with control of the mirror angles on the two launchers. The first traces in Figure 6 show the elongation reference, actual elongation, elongation error signal and gyrotron power.

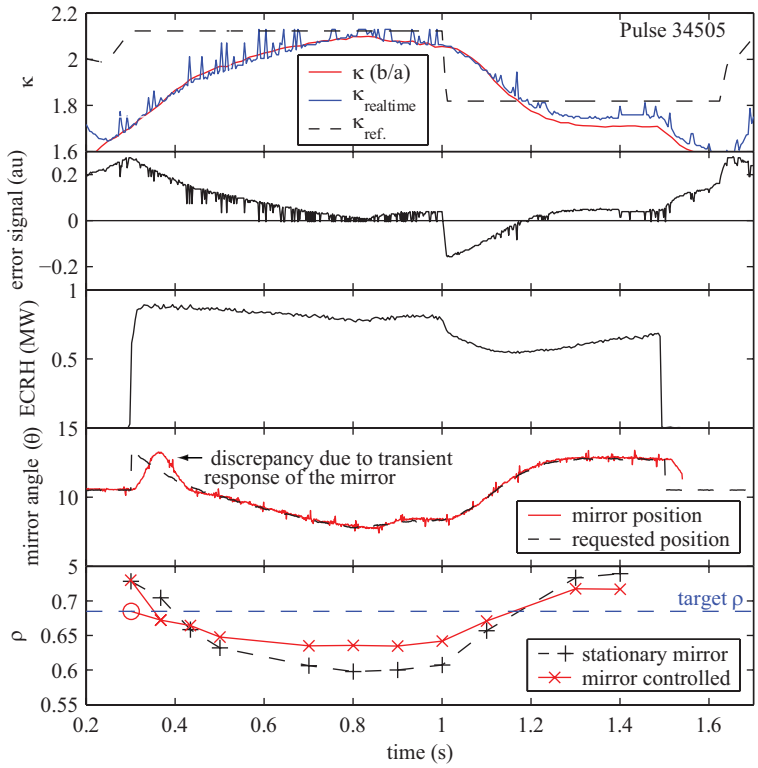

Figure 6. Real time control of the plasma elongation and ECRH deposition location. The reconstructed elongation trace is shown at the top of the figure together with $\kappa_{realtime}$ and the elongation reference signal. The error signal is the difference between the real time elongation signal and the elongation reference and is used in the ECRH power control algorithm only. ECRH power is switched on in a constant quadrupole field from 0.3s to 1.5s and the mirror control is also active during this time. The fourth trace shows the actuator signal for the mirror controller together with the measured mirror position. The TORAY-GA calculation of the deposition ρ is shown in the bottom trace (solid line) and compared with the expected deposition ρ given by a constant mirror angle at the feedforward value of 11.25deg (dashed line). The first point was also calculated under the assumption the mirror had moved immediately to the requested position (circle). The target ρ is also shown, which is simply the initial elongation at ECRH power-on.

Also shown in Figure 6 are the mirror angles as well as the centre of the deposition profiles at the given mirror angles, calculated from TORAY-GA (Gaussian fit of the deposition profiles centred at ρ). A slight discrepancy can be seen between the requested and the measured mirror angle at the feedback switch-on, which can be attributed to the transient response of the mirror. The corresponding deposition ρ (shown as a circle in the figure) was calculated assuming the mirror had moved to the requested location. As the elongation increases in the first phase from κ=1.8 to 2.1, the mirror is moved from θ=13 to 8 degrees which corresponds to deposition profiles roughly held between ($0.64<\rho<0.68$). In the second phase of the pulse when the elongation decreases, the mirror moves from 8deg to 13deg and the deposition moves from ρ=0.65 to ρ=0.72. Given a constant mirror angle of 11.25deg, the absorption would be initially centred at ρ=0.8 for κ=1.7 and would move to ρ=0.6 for κ=2.1. The control could be improved by using the above results, together with TORAY-GA, to calculate the mirror angles required to maintain the absorption at constant deposition ρ. A linearised

relation between θ and κ_realtime would then be obtained and the parameters entered into the controller for the subsequent pulse. There is also clearly some non-linearity in the deposition location, as after 1.2s, the deposition moves to ρ~0.7, despite the elongation being the same as at the beginning of the ECRH phase at 0.3-0.4s. The error in the $\kappa_{realtime}$ signal, shown in the first trace, was found to be too small to account for this and it is thought that changes in the plasma parameters, such as electron density and density profile are responsible.

3.3. Plasma current control

In the plasma current control experiments, ECRH was applied by all 6 X2 gyrotrons and the launcher angles optimised to provide ECCD. At ECRH switch-on, the Ohmic coil currents were set to be constant, providing zero loop voltage. The response to a step increase in the current reference signal, from ~157 to 186kA, can be seen in Figure 7 left. The error signal is given in matrix volts and the current in the Ohmic coils (transformer primary) is also shown to demonstrate the plasma current is fully non-inductive. At the step, the ECRH power increases to its saturated maximum at <3MW and the current responds in ~400ms. The power then slowly decreases as the error becomes smaller and the current approaches the reference value. Figure 7 right shows a pulse with a flat current reference signal in a 100kA discharge and a comparison with an open-loop case. The Ohmic coils are again clamped to constant current when ECRH power is applied at 0.4s and the plasma current then settles to ~100kA. The control loop shows a faster response to the initial reference current level, by switching the ECRH on at saturated low power. It then increases the power as the current approaches the reference and more effectively maintains the current towards the end of the pulse, despite the higher electron density (which reduces the ECCD efficiency) in this case, again by increasing the ECRH power from ~1.6s.

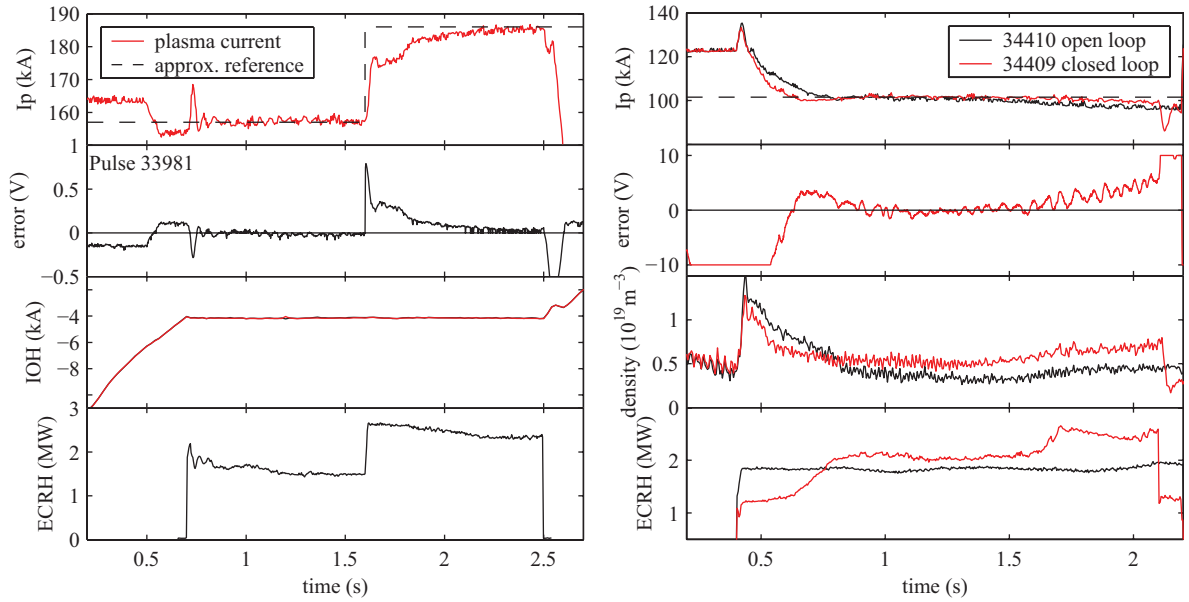

Figure 7 left. Plasma current control with a step increase in the current reference. The controller increases the ECRH power in response to the change in reference, driving more plasma current and minimising the error signal. Also shown is the current in the Ohmic coils which is flat during the control phase from 0.7 to 2.5s. Right. Comparison of open and closed loop (with a constant current reference) control cases. The control case responds faster to the initial reference and maintains a constant current for a longer time. Again the Ohmic coil currents are constant during the ECRH phase. There is a gyrotron arc at 2.2s, removing one cluster (half the available power).

4. Conclusions

In a constant quadrupole shaping field, the plasma elongation can be controlled by tailoring the plasma current profile using off-axis ECRH heating to modify the local resistivity. Therefore we have an actuator to control the plasma elongation. Real time control of the plasma elongation and of the location of the ECRH deposition was successfully demonstrated on TCV using gyrotron power and mirror actuators, a simplified real time elongation observer and a PID controller.

The ECRH deposition was tracked using movable ECRH mirrors and a prediction of the required deposition location from the plasma shape. The system was able to maintain an ECRH absorption profile centred at $\rho \sim 0.65$ ($0.64<\rho<0.68$) as the plasma elongated from $\kappa=1.8$ to 2.1. Simultaneous control of the elongation amplitude was successfully demonstrated using proportional-integral terms in the PID controller, a simplified elongation observer and control of the gyrotron power.

Plasma current control in fully non-inductive plasmas using ECCD to drive the current was also demonstrated, providing control of approximately 30kA of plasma current in discharges of 160kA by actuating the ECRH power level.

Elongation and current control would both benefit from a wider range of gyrotron power control, particularly at low gyrotron power, where the ability to switch the power entirely off would provide faster response to step-downs in either the current or elongation reference. With the imminent implementation of an entirely digital plasma controller, based on multiple Digital Signal Processors (DSP) [21], the potential for much more powerful algorithms will exist, including the ability to control the gyrotron power more effectively.

Acknowledgments

The authors would like to thank T.P. Goodman and Y. Camenen for useful discussions and F. Hofmann for the initial development of the elongation observers.

This work was funded by the European Atomic Energy Community under an intra-European fellowship (Euratom) and in part by the Swiss National Science Foundation.

Appendix. Real time calculation of the plasma elongation

There is at present no real time equilibrium reconstruction on the TCV tokamak. Typically the elongation kappa is calculated post-pulse by the equilibrium reconstruction code LIUQE (κ_{LIQUE}) [18]. In these experiments the plasma is modelled as a grid of 6 overlapping current filaments with current J_i and each with a triangular current profile [22]. A real time signal, related to the elongation is calculated by one of two methods 1) as a sum over the filaments of the quantity $J_i z_i^2$, where z is the

height of the current filament, or 2) based on a sum of fluxes on a fixed, predetermined boundary at the nominal plasma edge [23]:

$$\kappa_{realtime} = \psi_{up} + \psi_{down} - \psi_{left} - \psi_{right} \qquad \text{(A.1)}$$

Where ψ is the poloidal flux at pre-defined points (vertical and horizontal extrema) which lie on the last closed flux surface for a plasma with elongation of 2.2. When the plasma boundary (or a plasma flux surface) coincides with all of these points, $\kappa_{realtime}$ is zero and the elongation is 2.2. If the points do not lie on a flux surface, $\kappa_{realtime}$ is finite. The flux differences calculation was found to be more reproducible, especially as – unlike the Jz^2 method – it is insensitive to the plasma current profile, and so was used in the control. Each of these fluxes is given by

$$\psi_j = G_{ij} J_i \qquad \text{(A.2)}$$

Where index j = up, down, left, right and a summation over the repeated index i is implied. Fluxes are measured at a network of poloidal field coils within the vacuum vessel and flux loops on the surface of the vacuum vessel [24]. The fluxes measured by the coils and loops are given by:

$$\mu_k = F_{ik} J_i \qquad \text{(A.3)}$$

where μ_k is the flux at the k^{th} coil/loop and F is a matrix.

Therefore,

$$\psi_j = G_{ij} \left(F_{ik}^{-1} \mu_k \right) \qquad \text{(A.4)}$$

The matrix inversion is done in the least-squares sense.

The result is a quantity related to the elongation of the plasma, but which is not b/a (where b and a are the vertical and horizontal plasma radii, respectively). For finite $\kappa_{realtime}$, the error in $\kappa_{realtime}$ will be proportional to the plasma current, but as $\kappa_{realtime}$ is designed to be close to zero and we operate at constant current, the error is small. It also does not depend on position to first order as a rigid displacement should give no first order flux quadruple change. Again the plasma position, as well as shape (eg triangularity), minor radius etc are likely to be approximately constant and therefore it may be used as our real time elongation observable.

A comparison between the elongation (κ_{LIQUE} = b/a) and $\kappa_{realtime}$ may be seen in Figure 5 and Figure 6, which shows $\kappa_{realtime}$ linearly scaled and offset to match κ_{LIQUE}. The is a good match between the two signals, with only a small discrepancy towards the end of each pulse.

References

[1] O. Sauter et al., Physics of Plasmas 4 (1997) 1654-1664

[2] G. Gantenbein et al., Physical Review Letters 85 (2000) 1242-1245

[3] A. Manini et al., Proc. of the 14th Joint workshop on ECE and ECRH. EC-14 (2006) 44-53

[4] H. Zohm et al., Nuclear Fusion 47 (2007) 228-232

[5] D. A. Humphreys et al., Physics of Plasmas 13 (2006)

[6] J. Berrino et al., IEEE transactions on nuclear science 53 (2006) 1009-1014

[7] A. Isayama at al., Nucl. Fusion 43 (2003) 1272-1278

[8] ITER Physics Basis Nucl. Fusion 39 (Chapter 2) 2175 (1999)

[9] M.A. Henderson et al., Journal of Physics: Conference Series 25 (2005) 143-150

[10] S. Alberti et al., Nuclear Fusion 45 (2005) 1224-1231

[11] A. Pochelon et al., Nuclear Fusion 41 (2001) 1663-1669

[12] O. Sauter et al., Physics of Plasmas. 8 (2001) 2199

[13] S. Coda et al, Plasma Phys. Control. Fusion 42 (2000) B311

[14] T.P. Goodman et al., Proc. 19th SOFT (1996) 565

[15] T.P. Goodman et al., to be published Fusion Science & Technology 2007

[16] J.B. Lister et al., Fusion Technology 32 (1997) 321

[17] P.F. Isoz et al., Proc. 16th Symp. Fusion Technology, London, UK. (1990)

[18] F. Hofmann & G. Tonetti Nuclear Fusion 28 (1988) 1871

[19] K. Matsuda, IEEE Trans. Plasma Sci. 17 (1989) 6

[20] Y. Camenen et al., to be published in Nuclear Fusion 2007

[21] B.P. Duval et al., IEEE Trans. Nucl. Sci. 53 (2006) 2179

[22] F. Hofmann and G. Tonetti, Nucl. Fusion 28 (1988) 519

[23] F. Hofmann et al., Nucl. Fusion 30 (1990) 2013

[24] J.M. Moret et al., Rev. Sci. Instrum. 69 (1998) 2333